JCI insight

Signaling through retinoic acid receptors is essential for mammalian uterine receptivity and decidualization

Yan Yin, … , Ramakrishna Kommagani, Liang Ma

JCI Insight. 2021. https://doi.org/10.1172/jci.insight.150254.

Research In-Press Preview **Reproductive biology**

Retinoic Acid (RA) signaling has long been speculated to regulate embryo implantation, because many enzymes and proteins responsible for maintaining RA homeostasis and transducing RA signals are tightly regulated in the endometrium during this critical period. However, due to lack of genetic data, it was unclear whether RA signaling is truly required for implantation, and which specific RA signaling cascades are at play. Herein we utilize a genetic murine model that expresses a dominant negative form of RA receptor specifically in female reproductive organs to show that functional RA signaling is fundamental to female fertility, particularly implantation and decidualization. Reduction in RA signaling activity severely affects the ability of the uterus to achieve receptive status and decidualize, partially through dampening follistatin expression and downstream activin B/BMP2 signaling. To confirm translational relevance of these findings to humans, human endometrial stromal cells (hESCs) were treated with pan-RAR antagonist to show that in vitro decidualization is impaired. RNAi perturbation of individual *RAR* transcripts in hESCs revealed that RARα in particular is essential for proper decidualization. These data provide direct functional evidence that uterine RAR-mediated RA signaling is crucial for mammalian embryo implantation, and its disruption leads to failure of uterine receptivity and decidualization resulting in severely compromised fertility.

Signaling through Retinoic Acid Receptors is Essential for Mammalian Uterine Receptivity and Decidualization

Yan Yin[1], Meade Haller[1], Sangappa B Chadchan[2, 3], Ramakrishna Kommagani[2, 3], Liang Ma[1,4]

[1] Division of Dermatology, Department of Medicine, Washington University School of Medicine, St. Louis, MO, 63110, USA.

[2] Department of Obstetrics and Gynecology, Washington University School of Medicine, St Louis MO, 63110, USA

[3]Center for Reproductive Health Sciences, Washington University School of Medicine, St Louis MO, 63110, USA

[4]Author for correspondence

Liang Ma

660 S. Euclid Ave Box 8123

St. Louis, MO 63110

314-454-8771

lima@wustl.edu

Key words: retinoic acid, RAR, uterine receptivity, decidualization, follistatin

Running title: Retinoic acid signaling regulates implantation

Conflict of interest statement: The authors have declared that no conflict of interest exists.

Abstract

Retinoic Acid (RA) signaling has long been speculated to regulate embryo implantation, because many enzymes and proteins responsible for maintaining RA homeostasis and transducing RA signals are tightly regulated in the endometrium during this critical period. However, due to lack of genetic data, it was unclear whether RA signaling is truly required for implantation, and which specific RA signaling cascades are at play. Herein we utilize a genetic murine model that expresses a dominant negative form of RA receptor specifically in female reproductive organs to show that functional RA signaling is fundamental to female fertility, particularly implantation and decidualization. Reduction in RA signaling activity severely affects the ability of the uterus to achieve receptive status and decidualize, partially through dampening follistatin expression and downstream activin B/BMP2 signaling. To confirm translational relevance of these findings to humans, human endometrial stromal cells (hESCs) were treated with a pan-RAR antagonist to show that in vitro decidualization is impaired. RNAi perturbation of individual *RAR* transcripts in hESCs revealed that RARα in particular is essential for proper decidualization. These data provide direct functional evidence that uterine RAR-mediated RA signaling is crucial for mammalian embryo implantation, and its disruption leads to failure of uterine receptivity and decidualization resulting in severely compromised fertility.

Significance Statement: Female infertility affects as many as 72 million individuals worldwide, with 10% of cases remaining unsolved after clinical investigation. Retinoic acid is the biologically functional metabolite of dietary vitamin A. The current study shows that in the event that the mammalian uterus cannot respond properly to retinoic acid, it cannot properly receive an otherwise healthy embryo for implantation, and pregnancy is unlikely to be achieved. A functional uterine response to retinoic acid is therefore critical for early pregnancy success.

Introduction

During early pregnancy, the mammalian endometrium responds to changing ovarian hormones and signaling cues from embryos. The endometrium undergoes extensive growth and differentiation to become appropriately receptive to the incoming blastocysts for implantation (1, 2). Commonly referred to as the "window of implantation", these complex endometrial events must happen in rapid succession in a short time frame in order to achieve a receptive phase. In the mouse, the implantation window starts the morning of 3.5 days post coitum (dpc, 0.5 dpc = 1200h of the day of vaginal plug), when fertilized eggs complete their development through the blastocyst stage and descend into the uterus. By this time, the receiving luminal epithelium (LE) ceases proliferation and initiates differentiation under the influence of rising progesterone (P4) and a small estradiol (E2) surge, while the underlying stromal cells undergo extensive proliferation and start to differentiate into morphologically and functionally distinct decidual cells. Toward the evening of 4.5 dpc, the implantation window closes and the uterus enters the refractory phase, during which embryos cannot implant. The rapid uterine changes that define the implantation window are tightly regulated by a network of signaling pathways orchestrated by hormones, growth factors, cytokines, and transcription factors. The importance of uterine receptivity genes is evidenced by the severe implantation and/or decidualization defects that occur in response to loss-of-function mutations (3-10).

Retinoic acid (RA), a physiologically active metabolite of its inactive precursor retinol (vitamin A), is essential for many biological processes including cell survival, differentiation and apoptosis (11). Vitamin A deficiency, as well as genetically disrupting RA function, leads to defects in the development of many organs and tissues, including the nervous system, kidney,

skeleton, heart, lung and urogenital tracts (12). RA exerts its biological functions mainly through binding to the nuclear RA receptors (RARs) facilitated by the Cellular Retinoic Acid-Binding Proteins (CRABPs), or less frequently, to the non-canonical Peroxisome Proliferator-Activated Receptor β/γ (PPAR β/γ) facilitated by Fatty Acid-Binding Protein 5 (FABP5). The ratio of intracellular lipid-binding proteins CRABP2:FABP5 tips the balance toward one signaling pathway or the other, which frequently have opposing effects (13). Both RARs and PPARs form heterodimers with Retinoid X Receptors (RXRs), and they regulate target gene expression by directly binding to RA response elements (RAREs) and peroxisome proliferator response elements (PPREs), respectively. In addition to these two signaling cascades, RA can also bind to cytoplasmic RARs and trigger rapid kinase phosphorylation, which in turn regulates downstream signaling events (14).

Previous studies have implicated RA signaling in regulating female fertility. In both the rodent and human endometrium, expressions of RA synthesizing (ALDHs/RALDHs) and metabolizing enzymes (CYP26), as well as RA-binding proteins that regulate its bioavailability (CRBPs/CRABPs/FABP5), are temporally and spatially controlled during early pregnancy (15-17), suggesting their involvement in uterine receptivity and embryo implantation. In addition, high expression of RA signaling receptors, including RARs, PPAR β/γ and RXRs, has been reported at implantation sites of human and rodent endometrium (17-19). In cultured human endometrial stromal cells (hESCs), gene silencing of CRABP2 and FABP5 by siRNA inhibits and promotes decidualization, respectively (20), suggesting that RA-RAR signaling favors decidualization. In seemingly contradictory in vitro data, treatment of RA at pharmacological levels in hESC culture appears to impair decidualization (17, 21). Given the complex genomic and

non-genomic downstream events elicited by RA in various tissues and the absence of any uterine data from genetic animal models, the definitive role of RA signaling in implantation requires clarification.

In the current study, we utilized a previously characterized mouse strain that carries the *RaraT403* truncated form of human *RARα* knocked in to the *Rosa26* locus to dissect the role of RA-RAR signaling in embryo implantation (22). Cre-mediated recombination removes the floxed-STOP sequence upstream of the *RaraT403*, resulting in expression of the dominant negative form of RARα (hereinafter referred to as *Rara*DN), and subsequent inhibition of endogenous RAR-mediated transcriptional regulation of target genes. We showed that functional RAR signaling is required for mammalian uterine receptivity and decidualization both in the mouse model and in cultured hESCs.

Results

*Rara*DN^{Pgr} Females Are Severely Subfertile

To generate mice with disrupted RA signaling in the female reproductive tracts, *Rara*DN$^{f/+}$ mice were mated to *Pgr*-Cre mice, resulting in offspring females carrying both alleles (*Rara*DN$^{f/+;}$ *Pgr*-Cre, hereafter referred to as *Rara*DN^{Pgr}) and littermate controls (CTRL, no *Pgr*-Cre). *Pgr*-Cre-mediated gene recombination in the uterus is first detected in the luminal and glandular epithelia starting at two weeks of age, and gradually expands to the stroma and myometrium (23). To assess disruption of RAR signaling, we examined the expression of several *Hox* genes, known direct downstream targets of RAR, in the uteri of ovariectomized CTRL and *Rara*DN^{Pgr}

mice **(Figure S1)**. Reduction in expression of the majority of the *Hox* genes in the *Rara*DN^{Pgr} uteri demonstrates that RAR signaling is successfully disrupted in these animals. Female fertility was evaluated by breeding test of wild-type males with either *Rara*DN^{Pgr} or CTRL females and tracking the number of litters and pups produced by each female for 200 consecutive days. Six out of seven *Rara*DN^{Pgr} females tested were completely sterile, producing zero litters over the span of seven months **(Figure 1A)**. The remaining *Rara*DN^{Pgr} female produced only two litters, each consisting of only one pup after a long hiatus post mating setup **(Figure 1A and B)**. *Rara*DN^{Pgr} females as a whole are therefore severely subfertile, producing significantly fewer litters and pups than controls **(Table 1,** $p=9.8\times10^{-9}$ and 7.2×10^{-9}, respective, n=5 for CTRL and n=7 for *Rara*DN^{Pgr}**)**. No apparent developmental and behavioral abnormalities were observed in the two pups born to the *Rara*DN^{Pgr} sterility escapee. Vaginal plugs were consistently observed in the *Rara*DN^{Pgr} females, ruling out the possibility of behavioral issues preventing mating. As these females never presented palpable pregnancies, early-stage pregnancy defects were suspected.

*Rara*DN^{Pgr} Females Exhibit Implantation Defects

Mouse embryo implantation occurs between 3.5 and 4.5 dpc, when blastocysts attach to the luminal epithelium which in turn triggers the underlying stromal cells to undergo decidualization. Successful implantation is accompanied by increased local vascular permeability, which can be visualized by tail-vein injection of Chicago blue dye. Distinct blue dots indicating implantation sites were easily detectable along the uterine horns of CTRL mice at 4.5 dpc **(Figure 1D, arrows**, 9.7±2.1, n=3), but were completely absent in the *Rara*DN^{Pgr} uteri **(Figure 1C, E,** 0.0±0.0, n=3, $p=0.0013$**)**.

Many factors, alone or in combination, can contribute to failed pregnancy at an early stage, including abnormal ovulation, irregular ovarian hormone levels, and poor uterine receptivity. Since *Pgr*-Cre is also active in the adult ovary, including corpora lutea and hCG-stimulated granulosa cells (23), it is essential to investigate whether disturbance of RA signaling affects ovarian functions. Evaluation of the *Rara*DN^{Pgr} ovaries at 3.5 dpc revealed normal histology with presence of multiple corpus lutea, which are the remnants of successfully matured vesicular follicles after ovulation **(Figure S2A, B)**. Morphologically normal blastocysts were recovered from *Rara*DN^{Pgr} females by flushing the oviducts and uterine horns at 3.5 dpc **(Figure S2A, inset)**, and no significant difference was observed in the number of retrieved blastocysts at this stage **(Figure S2C,** CTRL 8.5±3.5, n=3; vs. *Rara*DN^{Pgr} 6.5±2.1, n=3, p=0.27**)** indicating normal fertilization rates. In addition, evaluation of serum ovarian hormone levels at this stage by ELISA revealed no significant differences **(Figure S2D)**. Together these data indicate normal ovarian function in *Rara*DN^{Pgr} females.

***Rara*DN^{Pgr} Females Exhibit Uterine Receptivity Defects**

Successful embryo implantation depends on the achievement of uterine receptivity through a series of molecular, hormonal and morphological changes. In the 3.5 dpc mouse uterus, the luminal epithelium typically ceases proliferation under the influence of decreased estrogen (E2) and surging progesterone (P4) levels to prime for rapid remodeling and embryo embedding (24). Meanwhile, luminal epithelial cells turn off genes for apical-basal polarity like Cadherin1 (CDH1, a.k.a. E-cadherin) to allow attachment of trophoblast cells to their apical pole (25). To assess the status of uterine receptivity, we first examined gross uterine morphology at this stage

and found no overt abnormalities except for aberrant luminal closure **(Figure 1F, G)**. Uteri of control 3.5 dpc females exhibited typical signs of receptivity, i.e. halted epithelial proliferation evidenced by limited phospho-Histone H3 staining **(**pHH3**, Figure 1G)** and reduced CDH1 expression exclusively in the luminal epithelium **(Figure 1K, arrowheads)**. By contrast, the *Rara*DN^{Pgr} uteri sustained high LE proliferating activity **(Figure 1H, arrowheads)** and high CDH1 expression **(Figure 1J, arrowheads)** in the luminal epithelium, consistent with a pre- or non-receptive uterus.

Quantitative RT-PCR was performed to further interrogate expression of genes involved in uterine receptivity. Amphiregulin (*Areg*), a member of the epidermal growth factor family, is upregulated exclusively in the uterine epithelium at 3.5 dpc surrounding the embedding embryos in a P4-dependent manner (26). This up-regulation was absent in the *Rara*DN^{Pgr} mutant **(Figure 1L)**. Expression of early growth response gene 1 (*Egr1*), a zinc finger transcription factor that is crucial for cell proliferation and angiogenesis, was previously reported to be induced in the subluminal stroma surrounding the blastocysts (27), but it is barely detectable in the mutant uterus at 3.5 dpc. Previous studies in ovarian hormone-responsive cells including uterine epithelial cells have shown that E2 signaling can promote luminal epithelium cell proliferation by transactivating expression of the cell cycle gene cyclin D1 (*Ccnd1*), as well as facilitating its nuclear translocation (28, 29). *Rara*DN^{Pgr} uteri exhibit a marked increase in *Ccnd1* mRNA, which may contribute to the mutant's aberrant epithelial proliferation. Deregulation of transcription factors essential for uterine receptivity and embryo implantation was also evident in the *Rara*DN^{Pgr} uteri at 3.5 dpc, including those expressed in the epithelial compartment, such as Forkhead Box O1 (*Foxo1*) (30), and those exclusively expressed in the stroma, such as

Homeobox A10 (*Hoxa10*) *(31).* RNAscope in situ hybridization of *Foxo1* revealed that its elevation in the mutant is confined to the uterine epithelium **(Figure 1N, O)**. In addition, analysis of a subset of gold standard receptivity biomarkers used in customized endometrial receptivity arrays (ERA) for clinical endometrial evaluation in humans (32, 33) revealed markedly reduced expression of many receptivity biomarkers in the *Rara*DN^{Pgr} uteri during the peri-implantation period **(Figure S3)**. Even though many of these genes have been reported to be regulated by ovarian hormones, the changes we observed in the *Rara*DN^{Pgr} mutant are unlikely to be elicited soly by altered hormone signaling, because serum ovarian hormone level **(Figure S2)** as well as uterine expression of ovarian hormone receptors and some of their well-established targets remained unchanged **(Figure 1M)**. Immunofluorescence of ESR1 and PR further confirmed that the ovarian hormone receptors were expressed at normal locations and levels in *Rara*DN^{Pgr} females comparable to their wildtype counterparts **(Figure 1P-S)**.

Decidualization is Compromised in *Rara*DN^{Pgr} Females

Despite the absence of luminal closure, which is thought to help immobilize the embryos for implantation, blastocyst attachment appears to successfully occur in the *Rara*DN^{Pgr} uteri at 4.5 dpc **(Figure 2B, D)**, raising the possibility that failures in subsequent pregnancy events also contribute to the fertility defects. As we and others have previously reported (34, 35), during embryo attachment, strong CDH1 expression is only present in the apical poles of the uterine epithelium and barely detectable on the basal side **(Figure 2C, arrows)**. Interestingly, this polarized localization of CDH1 is absent in the *Rara*DN^{Pgr} uteri; strong CDH1 staining was observed on both sides **(Figure 2D, arrowheads)**. Following embryo attachment, fibroblastic uterine mesenchymal cells undergo decidualization. Decidualization is the rapid proliferation and

differentiation of these cells into morphologically distinct decidual cells, which provide a plethora of growth factors and cytokines to support embryo development and serve an immunoregulatory role during early pregnancy. To investigate whether decidualization is affected in the *Rara*DN^{Pgr} females, we first examined the expression of known decidualization markers during natural pregnancy in these mutants. Transcription factor heart-and neural crest derivatives-expressed transcript 2 (HAND2) plays a critical role in uterine receptivity and decidualization in the mouse, and its expression is induced in endometrial stromal cells starting at 3.5 dpc and increases over time (7, 36). It modulates stromal-epithelial communications through negative regulation of FGF signaling, and genetic ablation of *Hand2* in the mouse leads to female infertility largely due to decidualization failure (7, 36). Immunofluorescence revealed that HAND2 protein exhibits nuclear localization in the CTRL subepithelial stromal cells at 4.5 dpc **(Figure 2F, arrows)**, but its level is dramatically reduced and its nuclear localization undetectable in the mutant uterus **(Figure 2E)**. This reduction in *Hand2* levels is confirmed at the transcript level by qRT-PCR using RNA extracted from whole uterine tissues at 4.5 dpc **(Figure 2G)**. Expression of an array of genes involved in decidualization were evaluated by qRT-PCR, and mutant uteri exhibit significant decreases in the majority of them, including *Add2*, *Ereg*, *Gata2*, *Hbegf*, *Hsd11b1*, *Igfbp1*, *Lcn2*, *Prl* and *Wnt4*. Interestingly, a significant increase in the transcript level of *Lpar3* was observed in the mutant 4.5 dpc uterus. *Lpar3* encodes lysophosphatidic acid receptor 3, a G protein-coupled receptor for lysophosphatidic acid that fine-tunes the local balance of P4 and E2 signaling during implantation (37, 38). Together these results demonstrate a decidualization failure in *Rara*DN^{Pgr} females in the setting of natural pregnancy.

To rule out the potential involvement of defective embryo attachment and/or defective hormone regulation as a cause for decidualization failure, we performed an artificial decidualization assay. In mice, decidualization of uterine stromal cells can be achieved by intra-luminal oil injection into the uterine horns of ovariectomized and hormone-primed females followed by additional hormone treatments post induction. As shown in **Figure 3A and B**, disruption of RA signaling in *Rara*DN^{Pgr} uteri renders them non-responsive to decidual stimuli. Uterine weight gain due to stimuli was completely abolished **(Figure 3C)**, and differentiation markers like *Igfbp1*, *Prl* and alkaline phosphatase (AP) failed to be induced in the mutant uteri **(Figure 3 D-F)**. Genes encoding RA receptors as well as some known downstream RAR signaling targets showed differential expression in stimulated mutant uteri relative to controls **(Figure 3G)**. Significant reduction in transcript levels were observed in the mutants for RA receptors *Rara*, *Rarb*, *Rxra* and *Rxrg*, as well as RA targets *Cdx1*, *Gbx2*, *Mmp9* and *Prrx2*. On the other hand, stimulated mutant uteri exhibit drastic increases in mRNA levels for transcription factors *Msx1* and *Sox17* relative to control decidua. Expression of *Msx1* was previously reported to sharply decline following embryo attachment to prepare the uterus for implantation by modulating WNT and FGF signaling between the epithelial and stromal compartments (39). In addition, persistent *Msx1* expression was shown to be associated with uterine receptivity defects observed in *Lif*-/- mice (40). *Sox17* also plays critical roles during implantation through modulating the uterine transcriptome (41). Most of the genes assayed including some of the RA receptors **(Figure 4A)** and their downstream targets **(Figure 4B)** display the same trend of expression changes during the peri-implantation period of natural pregnancy in *Rara*DN^{Pgr} uteri. These findings provide further support that disrupted expression of RAR downstream targets likely contributes to the decidualization defect observed in the *Rara*DN^{Pgr} mutants. We stress however, that at present we

cannot exclude the possibility that the decidualization defect in these mutants is secondary to the observed uterine receptivity defect. Tissue-specific ablation of RA signaling in the implanting uterus is required to address this point.

Disrupted RAR-Signaling Leads to Reduced Follistatin and Aberrant Activin Signaling

During gene expression analysis, we observed a striking decrease in the expression of follistatin (*Fst*) in the *Rara*DN^{Pgr} at 3.5 dpc **(Figure 5A)**. This is of particular interest as previous studies revealed that *Fst* is a direct transcriptional target of RA signaling, containing RA responsive elements (RAREs) in its promoter region (42). Additionally, *Pgr*-Cre-mediated genetic deletion of *Fst* leads to female fertility defects very similar to our *Rara*DN^{Pgr} mutants (43). Accompanying the sharp reduction of *Fst*, expression of inhibin βb (*Inhbb*), components of activin B and downstream target of FST signaling, was significantly up-regulated **(Figure 5A)**. In the uterine-specific *Fst* knockout model, absence of FST and elevated activin B activity caused reduction in BMP signaling, especially BMP2, through the Activin-SMAD signaling pathway (43). In line with this notion, we observed a similar reduction in *Bmp2* expression at 4.5 dpc **(Figure 5B)**, as well as reduction in phospho-SMAD1/5/8 **(Figure 5C)** in *Rara*DN^{Pgr} mutants. RNAscope in situ hybridization was performed, which further confirmed the reduction of *Fst* and *Bmp2* in *Rara*DN^{Pgr} uterus. *Fst* transcript was detected throughout the CTRL uterus at 3.5 dpc **(Figure 5D)** but was barely detectable in the mutant **(Figure 5E)**. *Bmp2* transcript was detected exclusively in the subepithelial stromal cells in CTRL uterus at 4.5 dpc **(Figure 5F)**, and its expression was markedly reduced in the mutant **(Figure 5G)**. If the fertility defects observed in the *Rara*DN^{Pgr} mice are indeed caused primarily by the loss of *Fst* expression, one would expect the phenotype to be alleviated when FST is supplemented back to the mutant

uterus. To test this hypothesis, we isolated uterine stromal cells from 2.5 dpc mutants for in vitro culture and added recombinant mouse FST to the medium at various concentrations. Forty-eight hours after culture, expression of several decidualization markers is elevated by addition of FST; for *Bmp2* and *Igfbp1* these changes are dose-dependent **(Figure 5H)**. Similar restoration of decidual marker expression were observed in a uterine organ culture system where either BSA- or FST-soaked agarose beads were inserted into the lumens of 2.5 dpc *Rara*DN^{Pgr} uterine segments and allowed to culture in vitro for two days **(Figure 5I)**. To test whether FST is sufficient to rescue the mutant implantation defects in vivo, FST was administered systemically into 2.5 dpc *Rara*DN^{Pgr} females via tail vein injection. At 6.5 dpc, bulging regions along the uterine horns resembling implantation sites were observed in these mutants **(Figure 5J)**, although they appeared smaller than normal implantation sites at this developmental stage. Sections through the bulging regions revealed elevated *Bmp2* and *Hand2* transcripts **(Figure 5K and 5L, respectively)**, as well as extensive AP activity **(Figure 5M)**, indicating restored decidualization in the mutant by FST administration. However, histological analyses did not reveal any uterine closure or embryo presence, suggesting that other aspects of implantation, most likely uterine receptivity, cannot be rescued by FST alone. This partial rescue was observed in two out of three *Rara*DN^{Pgr} females tested, with two and three bulging sites in each animal, respectively. These data together demonstrate that RARs regulate uterine decidualization mainly through FST.

RAR Signaling Is Essential for Decidualization in hESCs

In our previous study, we engineered a fluorescent reporter hESC line and performed genome wide siRNA screening to identify genes required for normal decidualization (44). A total of 136

296 genes involved in the RA pathway were among the hits, including 29 that are upstream and 107
297 that are downstream of RAR signaling **(Figure S4)**. To investigate the role of RAR signaling in
298 human endometrium, we performed individual siRNA knockdown against the three human *RAR*
299 genes (*RARA, RARB,* and *RARG*) in hESCs. In particular, knocking-down *RARA* significantly
300 inhibits in vitro decidualization of the hESCs, evidenced by decreased expression of
301 decidualization markers *IGFBP1* and *PRL* **(Figure 6A)**. Successful knockdown of individual
302 *RAR* genes were confirmed by qRT-PCR **(Figure 6B)**. Interestingly, siRNA against *RARA* not
303 only reduced *RARA* expression by more than 80%, but also simultaneously resulted in significant
304 increases in *RARB* and *RARG* expression, likely due to a compensatory signaling feedback loop
305 **(Figure 6B)**. By contrast, knocking down *RARB* or *RARG* did not affect hESC decidualization,
306 nor did it elicit significant changes in the expression of other *RAR* genes **(Figure 6A, B)**.
307
308 To further dissect the involvement of RAR genes in implantation, we evaluated the expression of
309 RA receptor genes by qRT-PCR in both mouse uterus during the peri-implantation period and
310 decidualized hESCs. As shown in **Figure S5**, in both model systems, *Rara/RARA* and
311 *Rarg/RARG* are the most abundant isotypes among the *Rar/RAR* genes, whereas *Rxra/RXRA* and
312 *Rxrb/RXRB* are the predominantly expressed *Rxr/RXR* genes. Hormonal regulation of the
313 receptor genes was also examined in cultured hESCs **(Figure S6)**. Twenty-four hours of
314 exposure to MPA elevates *RARA* transcript level, and this effect is augmented by co-treatment of
315 E2+MPA, even though E2 alone does not elicit any changes. *RXRB,* on the other hand, is
316 induced and suppressed by E2 and MPA respectively, and co-treatment appears to counteract
317 each other and cancel out the effect. Expression levels of the other *RAR* and *RXR* genes are not
318 affected by hormone treatment within this time frame.

To further demonstrate dependency of human decidualization on RA signaling, hESCs were treated with a pan-RAR antagonist, AGN194310 (45), at increasing concentrations. As shown in **Figure 6C**, decidualization markers *IGFBP1* and *PRL* both exhibit a dose-dependent decrease in expression upon drug treatment. Expression of endogenous *RAR* genes, including *RARA*, *RARG*, *RXRA* and *RXRB*, also exhibits dose-dependent reductions in response to AGN194310 **(Figure 6D)**. Taken together, these results strongly support the notion that RAR signaling, particularly through RARA, is required for in vitro decidualization of hESCs.

Discussion

In the current study, we generated and characterized a mouse model with conditional disruption of RA-RAR signaling specifically in female reproductive organs. The dominant negative *Rara*DN allele used in this study has been previously shown to block endogenous RAR-dependent signaling through competitively binding to RAREs (22). The vast majority of females carrying only one copy of the *Rara*DN allele in *Pgr*-cre-expressing cells are sterile, whereas one is severely subfertile, due to defective uterine receptivity and decidualization. Given that the dominant negative receptor blocks RAR signaling in a dose-dependent manner, and that having two alleles of *Rara*DN completely abolishes endogenous RA signaling (22), we expect the detrimental effects on female fertility would be more severe in *Pgr*-cre; *Rara*DN$^{flox/flox}$ females. Our findings also indicate that RA signaling through PPARβ/γ and/or non-genomic pathways cannot compensate for the loss of RAR signaling during implantation.

Even though *Pgr*-cre also mediates *Rara*DN expression in the ovary, there is no indication that the mutant ovaries are affected. Not only do ovarian hormone levels remain unchanged in these mutants, ovulation and fertilization also occur normally. Consistent with our data, genetic ablation of all three *Rar* genes as well as that of all three RA synthesis enzymes (*Aldh1a1-3*) in the developing mouse ovary, does not affect ovary differentiation or ovarian function (46). RAR signaling endogenous to the embryos also does not appear to be required for uterine receptivity or decidualization, as transgenic embryos carrying the *Rara*DN allele driven by an SV40 early promoter implant and develop to term when transferred into wild-type recipient dams (47).

In the absence of ligand, RAR/RXR heterodimers can actively repress target genes by occupying RAREs and complexing with corepressor proteins, such as nuclear-receptor corepressor (NCoR) and silencing mediator of retinoic acid (SMRT), to prevent transcription (48-50). Presence of RA induces conformational changes in the ligand-binding domain of RARs, resulting in simultaneous attenuation of affinity for co-repressors and increased affinity for co-activators, including histone acetyltransferases (HATs) and DRIP/TRAP/ARC coactivators and other mediator-containing complexes, to decompress chromatin and transactivate target genes (51-53). Rapid repression of target genes upon RA signaling activation has also been reported extensively (54-56), however the molecular mechanism is less studied. It is believed that liganded heterodimers recruit polycomb repressive complex 2 (PRC2), HDAC and co-regulator(s) to actively inhibit target gene transcription, but the identity of the co-regulator(s) remains unknown. Even though the three RAR genes share extensive homology and in many cases function redundantly, unliganded heterodimers RXR/RARβ and RXR/RARγ interact with SMRT co-repressors differently from unliganded heterodimers of RXR/RARα by mediating a substantial

level of transactivation rather than repression (57). The *Rara*DN mutant receptor used in this study lacks the carboxyl terminal sequence of the human *RARA* gene, but is also highly efficient at inhibiting the other two receptors (47). Dose-dependent blocking of transcription activation by this receptor has been demonstrated in various RARE-reporters both in vitro and in vivo (22, 47, 58), however, little is known about its impact on relieving repression or active inhibition of target genes. In the current study, we identified genes that are activated or repressed during the peri-implantation window in *Rara*DN^{Pgr} uterus, suggesting both instructive and permissive roles of RAR signaling. Whether these genes are direct transcriptional targets of RAR signaling, or their expression reflects a manifestation of changes in a cohort of "master RAR targets", demands further investigation.

In this study, we reported that the receptivity and decidualization defects in the *Rara*DN^{Pgr} uterus were partially caused by loss of *Fst* expression. FST, also known as activin-binding protein, is a glycoprotein that regulates of TGF-β superfamily signaling, primarily through binding to activin (59). Activin B, homodimer of Inhibin βB, binds to and activates ACVR2A/B and ALK4/7 and in turn phosphorylates SMAD2/3. *Fst* is upregulated during peri-implantation in the mouse uterus, which is believed to sequester activin B in order to allow BMP signaling activation (43). Genetic ablation of *Fst* leads to severe female subfertility in mice with receptivity and decidualization defects similar to *Rara*DN^{Pgr} mice (43), and aberrant expression of FST and activins are associated with poor pregnancy outcome in IVF patients (60). In *Rara*DN^{Pgr} mice, greatly reduced *Fst* expression was accompanied by increased *Inhbb* expression at 3.5 dpc and loss of *Bmp2* induction at 4.5 dpc. Interestingly the loss of *Bmp2* and deregulation of other decidualization markers were partially rescued by supplementation of FST protein in isolated

mutant endometrial stromal cells, in organ culture, as well as in vivo, suggesting that loss of FST can largely account for the severity of decidualization defects in *Rara*DN^{Pgr} mice. However, *Fst* down-regulation is unlikely to be the sole reason for the mutant impaired fertility for three reasons. First, gene expression changes in the *Rara*DN^{Pgr} mutants including a wide array of known RA targets were evident that have no known link to the FST and activin signaling pathway. Second, the fertility defects, especially in terms of decidualization, are much more severe in the *Rara*DN^{Pgr} mutants than in the *Fst*-cKO mice. Finally, not all decidualization genes tested were rescued by FST supplementation, e.g. *Prl*. Thus, while FST is an important downstream component of decidual RAR signaling, and while it is likely a direct RAR transcriptional target (42), our findings suggest that a wider network of signaling pathways is at play. Interestingly, regulation of BMPs by RAR signaling has been reported in other cellular contexts. In the mouse testicular embryonal carcinoma cell line, RA induces *Bmp2*, while simultaneously repressing *Bmp4*, specifically through RARα and γ (61). In primary bone marrow stromal cultures, addition of retinaldehyde stimulates *Bmp2* expression, and this induction is dampened by co-treatment of RAR antagonist AGN193109 (62). Whether the regulation of BMPs by RAR signaling is also mediated by FST in these specific cell types is not clear.

In addition to the mouse data, we also demonstrated the requirement of RAR signaling, specifically through RARα, in hESC decidualization. Knocking-down *RARA* in hESCs resulted in significant down-regulation of decidualization markers, as well as elevation of *RARB/G*, possibly by a compensatory mechanism in response to loss of RARα signaling. Knockdown of *RARB/G*, on the other hand, had no detectable effects on human in vitro decidualization. Treatment of a pan-RAR antagonist also caused a dose-dependent reduction of decidualization

marker expression, as well the expression of major *RAR/RXR* genes. Infertility due to vitamin A deficiency has been reported in humans, and fertility was restored after carefully titrated supplementation of Vitamin A back to normal levels (63). A review of the vitamin A content of the top 25 best-selling prenatal vitamins at the USA's top-grossing online store (amazon.com) revealed that the percent daily value for pregnant and nursing individuals ranges from 0% to 185% from a variety of precursors, with the topmost best-seller having no vitamin A **(Table S1)**. Extreme excess maternal vitamin A is a documented teratogen, although this is shown to be largely from feedback inhibition of native retinoic acid production in developing embryos (64). Low maternal vitamin A intake can likewise cause birth defects such as diaphragmatic hernia (65). The current study adds to the existing body of data to emphasize that not only is it essential for maternal/fetal health to have biologically appropriate levels of maternal RA, but it is also crucial for uterine receptivity and decidualization to have proper RA receptor signaling, as shown herein in mice in vivo and in hESCs in vitro.

Materials and Methods

Mice

Generation of mice carrying *Rara*DN preceded by a floxed transcriptional/translational STOP sequence was described previously (22), and cryopreserved sperms from mutant mice were provided by Dr. Benjamin D Humphreys in the Division of Nephrology, Washington University School of Medicine. Live mice carrying the *Rara*DN mutation were rederived via in vitro fertilization (IVF) at the Mouse Genetics Core at Washington University. Pgr-Cre line was provided by Dr. Francesco DeMayo at the National Institute of Environmental Health Sciences (23) and were mated to *Rara*DN$^{f/+}$ mice to generate offspring carrying both alleles (hereinafter

referred to as *Rara*DN^{Pgr}) and littermate controls (*Rara*DN$^{f/+}$, CTRL). Artificial decidualization and tail vein injection were performed following standard procedures as described previously (35, 66, 67). All mice used in this study were maintained in a barrier facility at Washington University School of Medicine, Missouri, following the institution's regulations with an approved protocol.

Uterine Stromal Cell Isolation and Organ Culture

Uteri of 2.5 dpc mice were collected, rinsed in cold Hank's Balanced Salt Solution (HBSS, Gibco), cut into 2-3mm pieces, and digested in 1% trypsin (Sigma) in HBSS for 1 hour at RT with gentle shaking. After incubation, luminal epithelium of each uterine segment was gently squeezed out using fine forceps along the longitudinal axis of the uterus. The remaining uterine tissues were transferred to a fresh tube, further digested in 0.25% trypsin and 1 mg/ml collagenase (Sigma) in HBSS for 30 min at 37 ºC with gentle shaking and dissociated by pipetting several times following incubation. Cell suspension and tissue remnants were filtered through a 70 µm nylon filter, and stromal cells were resuspended in hESC culture media (phenol red-free DMEM/F12, 7.5% charcoal-stripped FBS, 1x non-essential amino acids, 1x antibiotic-antimycotic). Stromal cells were seeded in 12-well plates, and follistatin (Sino Biological US Inc) were added to the culture media at indicated concentrations. For organ culture, 2.5 dpc uteri were cut into 2-3mm segments and placed on the membrane of multiwall inserts. The inserts were then placed into 12-well culture plates containing 0.5 ml culture medium, and ten agarose beads soaked in 100 ng/µl follistatin (Sino Biological US Inc., PA) or BSA were transferred into the lumen of each segment (68). Both primary stromal cells and uterine organ cultures were harvested 48 hours after for RNA isolation.

Human Endometrial Stromal Cell (hESC) Culture

Immortalized hESCs were characterized previously (69) and purchased from ATCC (the American Type Culture Collection, #CRL-4003). hESCs were maintained in hESC culture media plus 1x Insulin/Transferrin/Selenium (ITS, Gibco) in a humidified 37ºC incubator supplied with 5% CO_2. To induce decidualization in vitro, culture medium was replaced with induction medium (hESC medium plus 36 nM 17β-estradiol, 1 μM medroxyprogesterone/MPA, 0.1 mM cAMP) and hESCs were allowed to decidualize for 96 hours before RNA extraction. Gene-knockdown experiments were performed using DharmaFECT4 transfection reagent (GE Healthcare Dharmacon, Inc.) and Silencer™ Select Validated siRNAs (ThermoFisher, Cat# 4427038, *RARA*, siRNA ID# s11801; *RARB*, siRNA ID# s534565; *RARG*, siRNA ID# s11807) following manufacturer's instructions. The morning following transfection, 10x induction cocktail topper was added to the culture to a final concentration of 1x and cells were cultured for an additional 72 hours before harvest. For RAR-antagonist treatment, hESCs were treated with induction medium with or without AGN194310 (Sigma) at indicated concentrations for 72 hours, before harvest for RNA extraction.

RNA Isolation and Real-time RT-PCR

RNA was extracted in RNA STAT-60 reagent following manufacturer's instructions (Tel Test Inc). Reverse transcription was performed using the High Capacity cDNA Reverse Transcription kit (Applied Biosystems Inc., ABI), and qPCR performed on ViiA 7 Real-Time PCR System (ABI) using PowerUp™ SYBR™ Green Master Mix (ABI). All results were repeated in three

biological replicates unless specified and relative gene expression changes were determined by delta-delta Ct method (normalized to housekeeping gene, *Rpl7*). Primers are listed in **Table S2**.

Histology, Immunofluorescence (IF) and Alkaline Phosphatase (AP) Activity Assay

Tissue fixed in Bouin's fixative were processed for serial dehydration and embedding at the Developmental Biology Histology Core at Washington University School of Medicine. Eight micron paraffin sections were used for hematoxylin-eosin (H&E) staining and immunofluorescence (70). All antibodies were used at 1:1000 dilution in blocking solution (1% BSA, 3% normal goat serum in PBS): CDH1 (BD biosciences, San Jose, CA), phospho-Histone H3 (Millipore), Alexa594 goat anti-rabbit and Alexa488 goat anti-mouse (Life Technologies Corp., Carlsbad, CA). Paraformaldehyde (PFA)-fixed paraffin-embedded sections were used for AP activity assay. The sections were dewaxed, rehydrated and washed in PBS. Rehydrated sections were subsequently incubated in freshly-prepared AP staining solution containing 0.33 mg/ml NBT (nitro blue tetrazolium, Roche), 0.165 mg/ml BCIP (5-bromo-4-chloro-3-indolyl-phosphate, Roche) in AP buffer (100mM Tris-Cl, pH 9.0, 150mM NaCl, 1mM $MgCl_2$) for color development. Antibody catalog numbers are listed in **Table S3**.

Ovarian Hormone Analyses

Whole blood was collected by cardiac puncture and allowed to coagulate in 1.5ml Eppendorf tubes at room temperature for 20 minutes. The blood samples were centrifuged at 3000 rpm for 10 min at 4°C, and supernatant (serum) aliquoted and stored at -80°C until use. Cayman Chemical ELISA kits for detection of E2 (No. 501890) and P4 (No. 582601) were used to determine serum hormone levels, following manufacturer's instructions. Plates were read on a

Bio-Rad 3550 microplate reader at the wavelength of 405nm, data processed in Microsoft Excel and visualized in Graphpad Prism. Four biological replicates were tested and presented for each genotype.

In Situ Hybridization

In Situ hybridization was performed on PFA-fixed paraffin-embedded 8 μm tissue sections using RNAscope® 2.5 HD Assay-RED kit (Advanced Cell Diagnostics, ACD, Newark, CA). Gene-specific double-"Z" oligo probes compatible with the kit were ordered from ACD (probe-Mm-*Bmp2*, Cat# 406661; probe-Mm-*Fst*, Cat# 454331) and detailed in situ procedure has been described previously (35).

Statistical Analysis

All experimental groups contained three biological replicates, if not specified otherwise. Two-tailed Student's *t*-test assuming unequal variance was performed to compare means of the experimental groups. For dose response experiments, one-way ANOVA with post-hoc Tukey HSD test was performed. Data are presented as mean ± SD, with raw individual experimental data displayed as dot plots overlay, and *p*-value less than 0.05 was considered statistically significant.

Study Approval

The animal studies included herein were reviewed and approved by the Institutional Animal Care and Use Committee of Washington University in St. Louis, Missouri, USA. All studies were

performed to the current standards of the American Association for Laboratory Animal Science so as to minimize pain, suffering, and total animals necessary for conclusive findings.

Author contributions

YY, MH, and LM designed the study. YY, MH, and SBC conducted experiments. YY, MH, SBC, RK, and LM analyzed data and wrote the manuscript.

Acknowledgements

We thank Dr. Benjamin D Humphreys (Division of Nephrology, Washington University School of Medicine, St. Louis, MO) and Dr. Francesco DeMayo (National Institute on Environmental Health Sciences, Durham, NC) for providing cryopreserved sperm of *Rara*DN mutant mice and *Pgr*-Cre mice, respectively. We thank the Mouse Genetics Core at Washington University for rederiving the mutant mice. This work was supported by National Institutes of Health Grants DK113642 and HD087973 (to L.M.) and F32HD100120 (to M.H.).

References

1. Yoshinaga K. A sequence of events in the uterus prior to implantation in the mouse. *J Assist Reprod Genet.* 2013;30(8):1017-22.
2. Cha J, and Dey SK. Cadence of procreation: orchestrating embryo-uterine interactions. *Semin Cell Dev Biol.* 2014;34:56-64.
3. Wetendorf M, and DeMayo FJ. The progesterone receptor regulates implantation, decidualization, and glandular development via a complex paracrine signaling network. *Mol Cell Endocrinol.* 2012;357(1-2):108-18.
4. Pawar S, Laws MJ, Bagchi IC, and Bagchi MK. Uterine Epithelial Estrogen Receptor-α Controls Decidualization via a Paracrine Mechanism. *Mol Endocrinol.* 2015;29(9):1362-74.
5. Ma L, Yao M, and Maas RL. Genetic control of uterine receptivity during implantation. *Semin Reprod Endocrinol.* 1999;17(3):205-16.
6. Lee K, Jeong J, Kwak I, Yu CT, Lanske B, Soegiarto DW, et al. Indian hedgehog is a major mediator of progesterone signaling in the mouse uterus. *Nat Genet.* 2006;38(10):1204-9.

7. Li Q, Kannan A, DeMayo FJ, Lydon JP, Cooke PS, Yamagishi H, et al. The antiproliferative action of progesterone in uterine epithelium is mediated by Hand2. *Science.* 2011;331(6019):912-6.
8. Franco HL, Dai D, Lee KY, Rubel CA, Roop D, Boerboom D, et al. WNT4 is a key regulator of normal postnatal uterine development and progesterone signaling during embryo implantation and decidualization in the mouse. *FASEB J.* 2011;25(4):1176-87.
9. Monsivais D, Clementi C, Peng J, Titus MM, Barrish JP, Creighton CJ, et al. Uterine ALK3 is essential during the window of implantation. *Proc Natl Acad Sci U S A.* 2016;113(3):E387-95.
10. Curtis Hewitt S, Goulding EH, Eddy EM, and Korach KS. Studies using the estrogen receptor alpha knockout uterus demonstrate that implantation but not decidualization-associated signaling is estrogen dependent. *Biol Reprod.* 2002;67(4):1268-77.
11. Cunningham TJ, and Duester G. Mechanisms of retinoic acid signalling and its roles in organ and limb development. *Nat Rev Mol Cell Biol.* 2015;16(2):110-23.
12. Rhinn M, and Dollé P. Retinoic acid signalling during development. *Development.* 2012;139(5):843-58.
13. Schug TT, Berry DC, Shaw NS, Travis SN, and Noy N. Opposing effects of retinoic acid on cell growth result from alternate activation of two different nuclear receptors. *Cell.* 2007;129(4):723-33.
14. Al Tanoury Z, Piskunov A, and Rochette-Egly C. Vitamin A and retinoid signaling: genomic and nongenomic effects. *J Lipid Res.* 2013;54(7):1761-75.
15. Zheng WL, Sierra-Rivera E, Luan J, Osteen KG, and Ong DE. Retinoic acid synthesis and expression of cellular retinol-binding protein and cellular retinoic acid-binding protein type II are concurrent with decidualization of rat uterine stromal cells. *Endocrinology.* 2000;141(2):802-8.
16. Vermot J, Fraulob V, Dolle P, and Niederreither K. Expression of enzymes synthesizing (aldehyde dehydrogenase 1 and reinaldehyde dehydrogenase 2) and metabolizaing (Cyp26) retinoic acid in the mouse female reproductive system. *Endocrinology.* 2000;141(10):3638-45.
17. Ozaki R, Kuroda K, Ikemoto Y, Ochiai A, Matsumoto A, Kumakiri J, et al. Reprogramming of the retinoic acid pathway in decidualizing human endometrial stromal cells. *PLoS One.* 2017;12(3):e0173035.
18. Fukunaka K, Saito T, Wataba K, Ashihara K, Ito E, and Kudo R. Changes in expression and subcellular localization of nuclear retinoic acid receptors in human endometrial epithelium during the menstrual cycle. *Mol Hum Reprod.* 2001;7(5):437-46.
19. Ding NZ, Ma XH, Diao HL, Xu LB, and Yang ZM. Differential expression of peroxisome proliferator-activated receptor delta at implantation sites and in decidual cells of rat uterus. *Reproduction.* 2003;125(6):817-25.
20. Pavone ME, Malpani S, Dyson M, and Bulun SE. Altered retinoid signaling compromises decidualization in human endometriotic stromal cells. *Reproduction.* 2017;154(3):207-16.
21. Brar AK, Kessler CA, Meyer AJ, Cedars MI, and Jikihara H. Retinoic acid suppresses in-vitro decidualization of human endometrial stromal cells. *Mol Hum Reprod.* 1996;2(3):185-93.

22. Rosselot C, Spraggon L, Chia I, Batourina E, Riccio P, Lu B, et al. Non-cell-autonomous retinoid signaling is crucial for renal development. *Development.* 2010;137(2):283-92.
23. Soyal SM, Mukherjee A, Lee KY, Li J, Li H, DeMayo FJ, et al. Cre-mediated recombination in cell lineages that express the progesterone receptor. *Genesis.* 2005;41(2):58-66.
24. Dey SK, Lim H, Das SK, Reese J, Paria BC, Daikoku T, et al. Molecular cues to implantation. *Endocr Rev.* 2004;25(3):341-73.
25. Thie M, Harrach-Ruprecht B, Sauer H, Fuchs P, Albers A, and Denker HW. Cell adhesion to the apical pole of epithelium: a function of cell polarity. *Eur J Cell Biol.* 1995;66(2):180-91.
26. Das SK, Chakraborty I, Paria BC, Wang XN, Plowman G, and Dey SK. Amphiregulin is an implantation-specific and progesterone-regulated gene in the mouse uterus. *Mol Endocrinol.* 1995;9(6):691-705.
27. Guo B, Tian XC, Li DD, Yang ZQ, Cao H, Zhang QL, et al. Expression, regulation and function of Egr1 during implantation and decidualization in mice. *Cell Cycle.* 2014;13(16):2626-40.
28. Prall OW, Sarcevic B, Musgrove EA, Watts CK, and Sutherland RL. Estrogen-induced activation of Cdk4 and Cdk2 during G1-S phase progression is accompanied by increased cyclin D1 expression and decreased cyclin-dependent kinase inhibitor association with cyclin E-Cdk2. *J Biol Chem.* 1997;272(16):10882-94.
29. Tong W, and Pollard JW. Progesterone inhibits estrogen-induced cyclin D1 and cdk4 nuclear translocation, cyclin E- and cyclin A-cdk2 kinase activation, and cell proliferation in uterine epithelial cells in mice. *Mol Cell Biol.* 1999;19(3):2251-64.
30. Adiguzel D, Sahin P, Kuscu N, Ozkavukcu S, Bektas NI, and Celik-Ozenci C. Spatiotemporal expression and regulation of FoxO1 in mouse uterus during peri-implantation period. *PLoS One.* 2019;14(5):e0216814.
31. Lim H, Ma L, Ma WG, Maas RL, and Dey SK. Hoxa-10 regulates uterine stromal cell responsiveness to progesterone during implantation and decidualization in the mouse. *Mol Endocrinol.* 1999;13(6):1005-17.
32. Díaz-Gimeno P, Horcajadas JA, Martínez-Conejero JA, Esteban FJ, Alamá P, Pellicer A, et al. A genomic diagnostic tool for human endometrial receptivity based on the transcriptomic signature. *Fertil Steril.* 2011;95(1):50-60, .e1-15.
33. Horcajadas JA, Pellicer A, and Simón C. Wide genomic analysis of human endometrial receptivity: new times, new opportunities. *Hum Reprod Update.* 2007;13(1):77-86.
34. Jha RK, Titus S, Saxena D, Kumar PG, and Laloraya M. Profiling of E-cadherin, beta-catenin and Ca(2+) in embryo-uterine interactions at implantation. *FEBS Lett.* 2006;580(24):5653-60.
35. Yin Y, Wang A, Feng L, Wang Y, Zhang H, Zhang I, et al. Heparan Sulfate Proteoglycan Sulfation Regulates Uterine Differentiation and Signaling During Embryo Implantation. *Endocrinology.* 2018;159(6):2459-72.
36. Huyen DV, and Bany BM. Evidence for a conserved function of heart and neural crest derivatives expressed transcript 2 in mouse and human decidualization. *Reproduction.* 2011;142(2):353-68.
37. Diao H, Li R, El Zowalaty AE, Xiao S, Zhao F, Dudley EA, et al. Deletion of Lysophosphatidic Acid Receptor 3 (Lpar3) Disrupts Fine Local Balance of Progesterone

and Estrogen Signaling in Mouse Uterus During Implantation. *Biol Reprod.* 2015;93(5):123.
38. Ye X, Hama K, Contos JJ, Anliker B, Inoue A, Skinner MK, et al. LPA3-mediated lysophosphatidic acid signalling in embryo implantation and spacing. *Nature.* 2005;435(7038):104-8.
39. Nallasamy S, Li Q, Bagchi MK, and Bagchi IC. Msx homeobox genes critically regulate embryo implantation by controlling paracrine signaling between uterine stroma and epithelium. *PLoS Genet.* 2012;8(2):e1002500.
40. Daikoku T, Song H, Guo Y, Riesewijk A, Mosselman S, Das SK, et al. Uterine Msx-1 and Wnt4 signaling becomes aberrant in mice with the loss of leukemia inhibitory factor or Hoxa-10: evidence for a novel cytokine-homeobox-Wnt signaling in implantation. *Mol Endocrinol.* 2004;18(5):1238-50.
41. Wang X, Li X, Wang T, Wu SP, Jeong JW, Kim TH, et al. SOX17 regulates uterine epithelial-stromal cross-talk acting via a distal enhancer upstream of Ihh. *Nat Commun.* 2018;9(1):4421.
42. Cunningham TJ, Colas A, and Duester G. Early molecular events during retinoic acid induced differentiation of neuromesodermal progenitors. *Biol Open.* 2016;5(12):1821-33.
43. Fullerton PT, Monsivais D, Kommagani R, and Matzuk MM. Follistatin is critical for mouse uterine receptivity and decidualization. *Proc Natl Acad Sci U S A.* 2017;114(24):E4772-E81.
44. Haller M, Yin Y, and Ma L. Development and utilization of human decidualization reporter cell line uncovers new modulators of female fertility. *Proc Natl Acad Sci U S A.* 2019;116(39):19541-51.
45. Tukiainen P, Nickels J, Taskinen E, and Nyberg M. Pulmonary granulomatous reaction: talc pneumoconiosis or chronic sarcoidosis? *Br J Ind Med.* 1984;41(1):84-7.
46. Minkina A, Lindeman RE, Gearhart MD, Chassot AA, Chaboissier MC, Ghyselinck NB, et al. Retinoic acid signaling is dispensable for somatic development and function in the mammalian ovary. *Dev Biol.* 2017;424(2):208-20.
47. Damm K, Heyman RA, Umesono K, and Evans RM. Functional inhibition of retinoic acid response by dominant negative retinoic acid receptor mutants. *Proc Natl Acad Sci U S A.* 1993;90(7):2989-93.
48. Hu X, and Lazar MA. The CoRNR motif controls the recruitment of corepressors by nuclear hormone receptors. *Nature.* 1999;402(6757):93-6.
49. Nagy L, Kao HY, Love JD, Li C, Banayo E, Gooch JT, et al. Mechanism of corepressor binding and release from nuclear hormone receptors. *Genes Dev.* 1999;13(24):3209-16.
50. Perissi V, Staszewski LM, McInerney EM, Kurokawa R, Krones A, Rose DW, et al. Molecular determinants of nuclear receptor-corepressor interaction. *Genes Dev.* 1999;13(24):3198-208.
51. Heery DM, Kalkhoven E, Hoare S, and Parker MG. A signature motif in transcriptional co-activators mediates binding to nuclear receptors. *Nature.* 1997;387(6634):733-6.
52. Torchia J, Rose DW, Inostroza J, Kamei Y, Westin S, Glass CK, et al. The transcriptional co-activator p/CIP binds CBP and mediates nuclear-receptor function. *Nature.* 1997;387(6634):677-84.

53. Glass CK, and Rosenfeld MG. The coregulator exchange in transcriptional functions of nuclear receptors. *Genes Dev.* 2000;14(2):121-41.
54. Savory JG, Edey C, Hess B, Mears AJ, and Lohnes D. Identification of novel retinoic acid target genes. *Dev Biol.* 2014;395(2):199-208.
55. Kim M, Habiba A, Doherty JM, Mills JC, Mercer RW, and Huettner JE. Regulation of mouse embryonic stem cell neural differentiation by retinoic acid. *Dev Biol.* 2009;328(2):456-71.
56. Akanuma H, Qin XY, Nagano R, Win-Shwe TT, Imanishi S, Zaha H, et al. Identification of Stage-Specific Gene Expression Signatures in Response to Retinoic Acid during the Neural Differentiation of Mouse Embryonic Stem Cells. *Front Genet.* 2012;3:141.
57. Hauksdottir H, Farboud B, and Privalsky ML. Retinoic acid receptors beta and gamma do not repress, but instead activate target gene transcription in both the absence and presence of hormone ligand. *Mol Endocrinol.* 2003;17(3):373-85.
58. Gandhi D, Molotkov A, Batourina E, Schneider K, Dan H, Reiley M, et al. Retinoid signaling in progenitors controls specification and regeneration of the urothelium. *Dev Cell.* 2013;26(5):469-82.
59. Ying SY. Inhibins, activins, and follistatins: gonadal proteins modulating the secretion of follicle-stimulating hormone. *Endocr Rev.* 1988;9(2):267-93.
60. Prakash A, Tuckerman E, Laird S, Ola B, Li TC, and Ledger WL. A preliminary study comparing the endometrial expression of inhibin, activin and follistatin in women with a history of implantation failure after IVF treatment and a control group. *BJOG.* 2008;115(4):532-6; discussion 6-7.
61. Rogers MB. Receptor-selective retinoids implicate retinoic acid receptor alpha and gamma in the regulation of bmp-2 and bmp-4 in F9 embryonal carcinoma cells. *Cell Growth Differ.* 1996;7(1):115-22.
62. Nallamshetty S, Wang H, Rhee EJ, Kiefer FW, Brown JD, Lotinun S, et al. Deficiency of retinaldehyde dehydrogenase 1 induces BMP2 and increases bone mass in vivo. *PLoS One.* 2013;8(8):e71307.
63. Kalampokas T, Shetty A, and Maheswari A. Journal of Women's Health Care; 2014.
64. Lee LM, Leung CY, Tang WW, Choi HL, Leung YC, McCaffery PJ, et al. A paradoxical teratogenic mechanism for retinoic acid. *Proc Natl Acad Sci U S A.* 2012;109(34):13668-73.
65. Rocke AW, Clarke TG, Dalmer TRA, McCluskey SA, Rivas JFG, and Clugston RD. Low maternal vitamin A intake increases the incidence of teratogen induced congenital diaphragmatic hernia in mice. *Pediatr Res.* 2021.
66. Behringer R, Gertsenstein M, Nagy KV, and Nagy A. *Manipulating the mouse embryo : a laboratory manual.* Cold Spring Harbor, New York: Cold Spring Harbor Laboratory Press; 2014.
67. Reese J, Binart N, Brown N, Ma WG, Paria BC, Das SK, et al. Implantation and decidualization defects in prolactin receptor (PRLR)-deficient mice are mediated by ovarian but not uterine PRLR. *Endocrinology.* 2000;141(5):1872-81.
68. Paria BC, Ma W, Tan J, Raja S, Das SK, Dey SK, et al. Cellular and molecular responses of the uterus to embryo implantation can be elicited by locally applied growth factors. *Proc Natl Acad Sci U S A.* 2001;98(3):1047-52.

729 69. Krikun G, Mor G, Alvero A, Guller S, Schatz F, Sapi E, et al. A novel immortalized human
730 endometrial stromal cell line with normal progestational response. *Endocrinology.*
731 2004;145(5):2291-6.
732 70. Yin Y, Lin C, and Ma L. MSX2 promotes vaginal epithelial differentiation and wolffian
733 duct regression and dampens the vaginal response to diethylstilbestrol. *Mol Endocrinol.*
734 2006;20(7):1535-46.
735

736

Table 1. 200-day Breeding Record

Genotype	Number of ♀ tested	Cumulative pups - total	Cumulative pups/female	Cumulative litters - total	Cumulative litters/female
CTRL	5	311	62.2	34	6.8
*Rara*DN^{Pgr}	7	2	0.286	2	0.286

Figure Legends

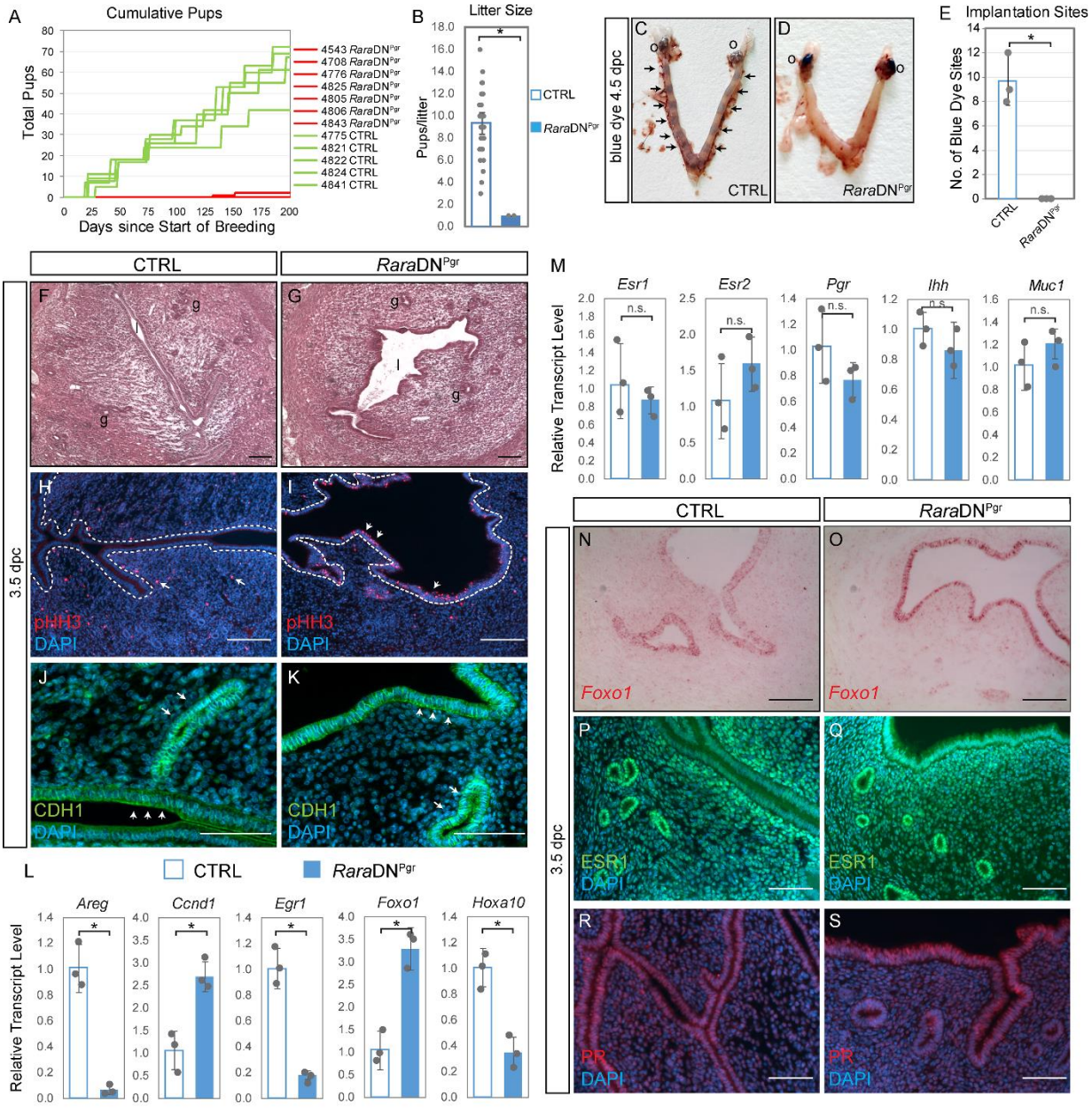

Figure 1. Impaired female fertility due to implantation failure in *Rara*DN^{Pgr} mice. (A)

Cumulative number of pups produced by individual CTRL (green) and *Rara*DN^{Pgr} females (red) over the period of 200 days. (B) Average number of pups per litter produced by the females presented in A. (C, D) Representative images of visualization of implantation sites (arrows) by Blue Dye injection at 4.5 dpc. O, ovaries. (E) Quantification of implantation sites from CTRL (9.7±2.1, n=3) and *Rara*DN^{Pgr} females (0.0±0.0, n=3, p=0.0013). (F, G) H&E staining of *Rara*DN^{Pgr} and CTRL uteri at 3.5 dpc. g, glands; l, lumen. (H, I) Immunofluorescence detecting pHH3-positive proliferating cells at 3.5 dpc (arrowheads, uterine epithelial cells; arrows, proliferating stromal cells; dashed lines outline the luminal epithelia). (J, K) CDH1 immunofluorescence on 3.5 dpc uterine sections. Note in the CTRL, reduced CDH1 level is obvious in the luminal epithelium (J, arrowheads) when compared to glandular epithelium (J, arrows); whereas this difference is negligible in *Rara*DN^{Pgr} uterus (K). (L, M) Gene expression at 3.5 dpc determined by qRT-PCR, normalized to levels of housekeeping gene *Rpl7* and the average transcript level of CTRL samples was set to one. (N, O) RNAscope in situ hybridization of *Foxo1* showing elevated transcript level in the mutant epithelium. (P-S) IF staining of ESR1 (P,Q) and PR (R,S) revealed no apparent differences in expression. *, p <0.05; n.s. not significant. Scale bars: 50µm.

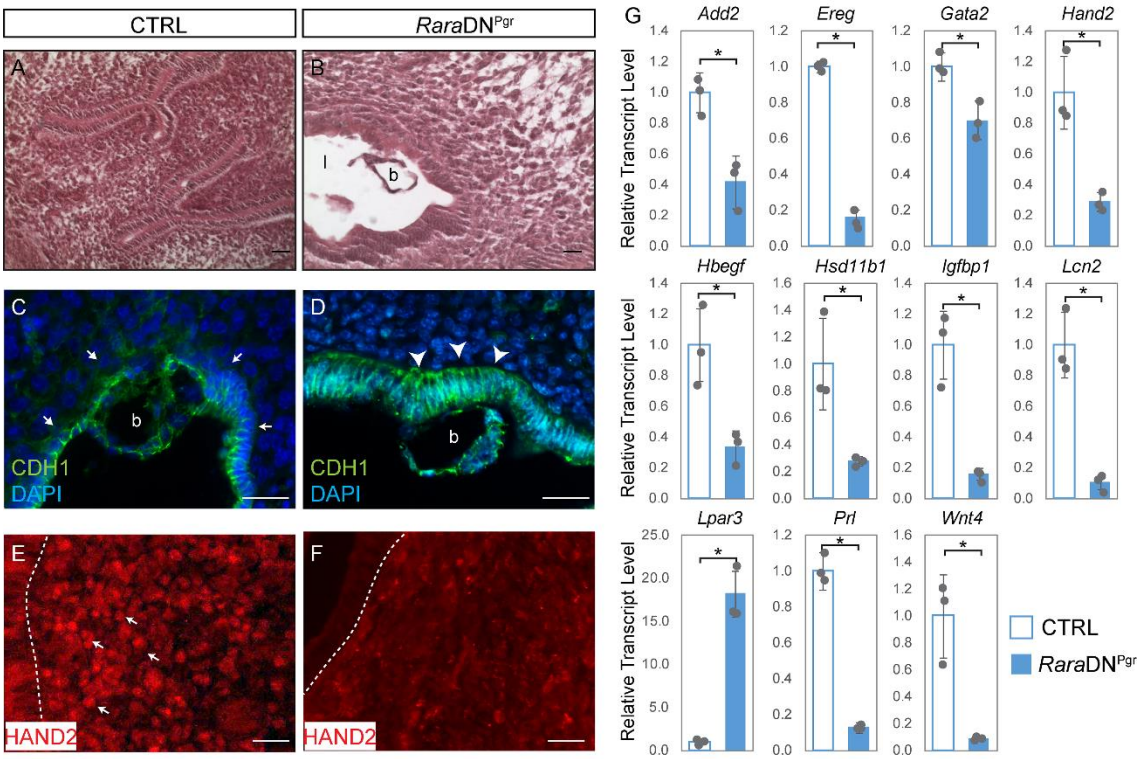

Figure 2. Failure of decidualization in 4.5 dpc *Rara*DN^{Pgr} uterus. (A, B) H&E staining of *Rara*DN^{Pgr} and CTRL uteri at 4.5dpc. l, lumen; b, blastocyst. (C, D) CDH1 immunofluorescence on 4.5dpc uterine sections. Note the presence of normal blastocyst in the mutant lumen (D), and persistent high CDH1 level in the underlying luminal epithelium especially at the basal side (arrowheads, compared to CTRL arrows in C). (E, F) Immunofluorescent detection of HAND2 protein in the nuclei of decidual cells in the CTRL (arrows, E), which is absent in the mutant (F). (G) Relative transcript levels of genes involved in decidualization by qRT-PCR. Scale bars: 50µm.

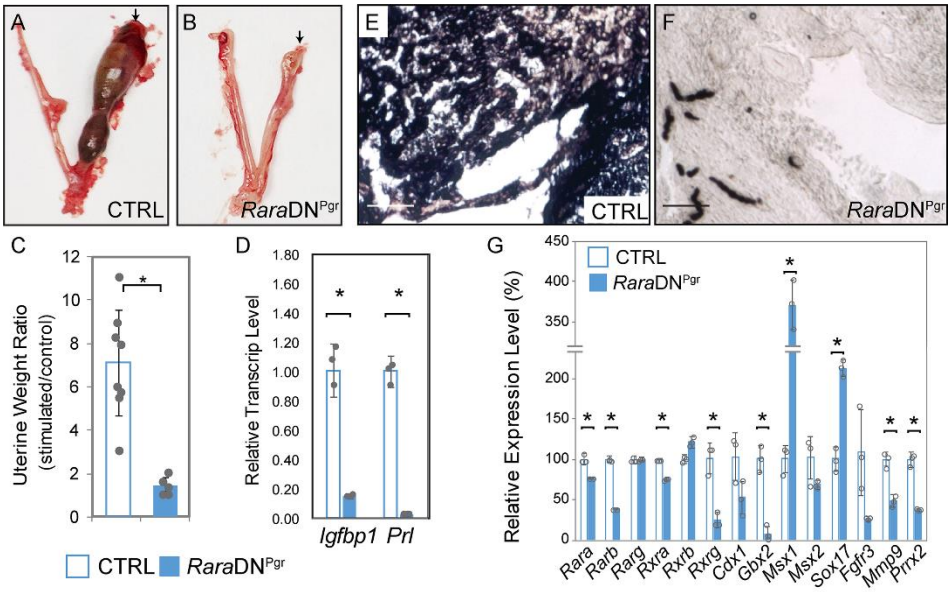

Figure 3. *Rara*DN^{Pgr} mutant uterus does not respond to artificial decidualization stimuli in vivo. (A, B) Representative images of artificially decidualized uteri five days after stimulation. Arrows indicate the uterine horn that received intrauterine oil infusion; contralateral horns serve as controls. (C) Uterine weight ratio (wet weight stimulated/wet weight unstimulated) was calculated for each animal, and graphed as mean ± SD (CTRL, 7.1 ± 2.4, n=8; RaraDNPgr, 1.4 ± 2.4, n=5; p=0.00036). (D) Gene expression data of decidualization markers, Igfbp1 and Prl, in the stimulated uterine horn by qRT-PCR. (E, F) Alkaline phosphatase activity in the stimulated uterine horns visualized by dark color development from AP substrate BCIP/NBT. (G) Gene expression analyses of RA receptors and RAR targets comparing RNA extracted from stimulated CTRL and *Rara*DN^{Pgr} uteri by qRT-PCR. Asterisks indicate p <0.05. Scale bars: 50µm.

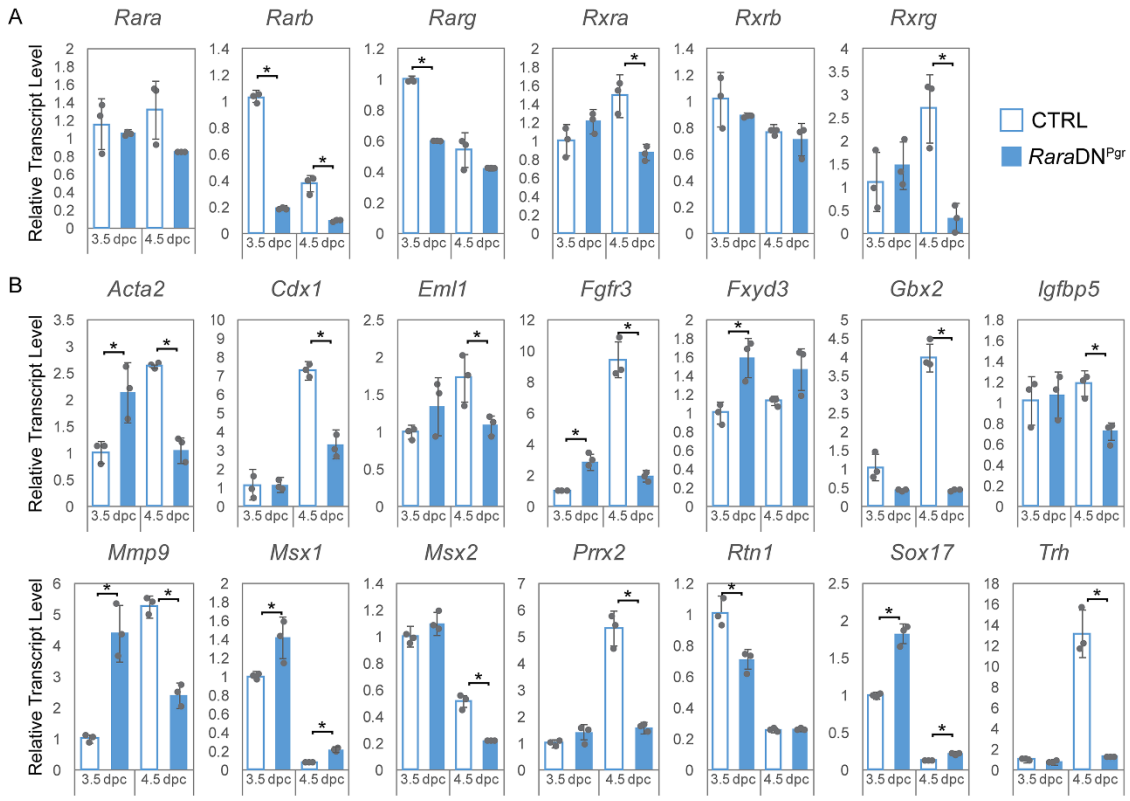

Figure 4. Changes in expression of RA receptor genes and known RAR targets in the *Rara*DN^{Pgr} uterus during the peri-implantation period. Gene expression by qRT-PCR performed on whole uterine RNA extract at 3.5 and 4.5 dpc detecting RA receptors (A) and targets (B). Asterisks indicate $p < 0.05$ comparing to CTRL uteri of same timepoint.

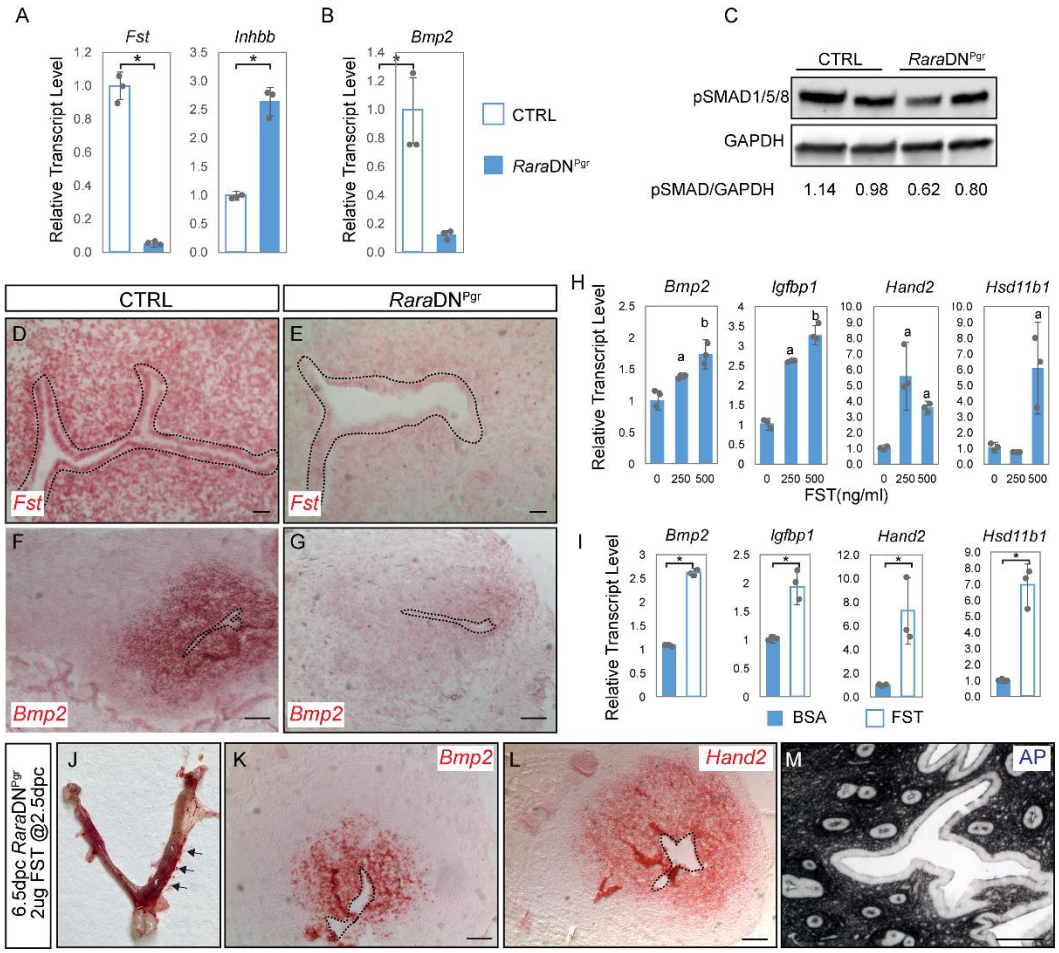

Figure 5. Reduced follistatin expression and downstream changes in activin/BMP signaling are partially responsible for the fertility defects in *Rara*DN^{Pgr} uterus. (A, B) Relative expression levels of Fst and Inhbb at 3.5 dpc (A), and Bmp2 at 4.5 dpc (B). (C) Western blot for phospho-Smad1/5/8 of whole uteri extract from CTRL and RaraDN^{Pgr} females at 3.5 dpc. WB band density was quantified in ImageJ and the relative density calculated as the ratio of pSMAD/GAPDH for each sample was listed. (D-G) RNAscope in situ hybridization of *Fst* at 3.5 dpc (D, E) and *Bmp2* at 4.5 dpc (F, G). Positive results manifest as red staining; dotted lines outline the luminal epithelium. (H) Gene expression of decidualization markers in isolated endometrial stromal cells from 2.5 dpc *Rara*DN^{Pgr} uteri treated with recombinant mouse FST at indicated concentrations for 48 hours (n=2). (I) Gene expression of decidualization markers in

uterine segments dissected from 2.5 dpc *Rara*DN^{Pgr} and incubated with luminal agarose beads soaked with BSA or FST for two days (n=2). (J) Appearance of *Rara*DN^{Pgr} mutant uteri four days after receiving 2 µg FST via tail vein injection (arrows point to bulging regions resembling implantation sites). (K-L) RNAscope in situ hybridization of *Bmp2* (K) and *Hand2* (L) showed elevated expression in the bulging region. (M) BCIP-NBP staining of bulging regions shows extensive alkaline phosphatase activity. Asterisks indicate p <0.05 by t-test; a indicates p <0.05 by one-way ANOVA between drug group and control group; and b indicates p <0.05 by one-way ANOVA between different doses. Scale bars: 50µm.

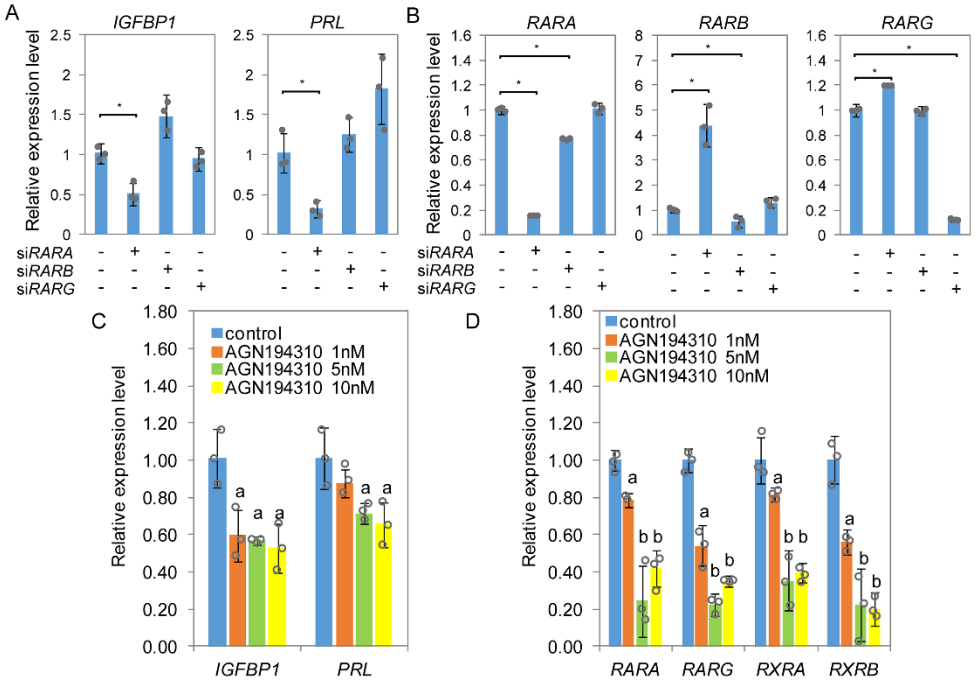

Figure 6. RAR signaling is essential for decidualization of hESCs. (A, B) Gene expression by qRT-PCR of human decidualization markers (A) and RAR genes (B) when individual RAR genes are silenced by siRNA. (C, D) Expression of decidualization markers (C) and selective RAR and RXR genes (D) when hESCs are treated with pan-RAR antagonist AGN194310 at indicated concentrations. Asterisks indicate p <0.05 by t-test; a indicates p <0.05 by one-way

811 ANOVA between drug group and control group; and b indicates $p < 0.05$ by one-way ANOVA

812 between different doses.

813